RAPID COMMUNICATIONS

PHYSICAL REVIEW A VOLUME 40, NUMBER 1 JULY 1, 1989

Barkas effect observed with antiprotons and protons

G. Gabrielse, X. Fei, L. A. Orozco, S. L. Rolston,* and R. L. Tjoelker
Department of Physics, Harvard University, Cambridge, Massachusetts 02138

T. A. Trainor
Department of Physics, University of Washington, Seattle, Washington 98195

J. Haas and H. Kalinowsky
Institut für Physik, Johannes Gutenberg-Universität Mainz, Postfach 3980, D-6500 Mainz, West Germany

W. Kells†
Fermi National Accelerator Laboratory, Batavia, Illinois 60510
(Received 8 February 1989)

The difference in the range of protons and antiprotons in matter, an example of the Barkas effect, is observed in a simple time-of-flight apparatus. The ranges of 5.9-MeV antiprotons and protons differ by about 6% in a degrader made predominantly of aluminum.

The availability of low-energy antiprotons has triggered experimental and theoretical interest in comparing the interaction of protons and antiprotons with matter. Two examples are the calculation of the excitation of atomic inner shells by antiprotons[1] and the measurement of different cross sections for the double ionization of helium by protons and antiprotons.[2] The latter prompted theoretical studies[3,4] which predict different distributions of secondary electrons when protons and antiprotons are incident on He. In this Rapid Communication we report a new measurement. Antiprotons and protons were sent through aluminum to directly measure the Barkas effect, a difference in range for particles differing only in the sign of charge. The Barkas effect is large, easily measurable, and seems to agree with more recent theories. The measurements were used to ensure reliable capture of antiprotons in an ion trap for mass spectroscopy[5] as part of an experimental effort in progress at the Low-Energy Antiproton Ring (LEAR) of the European Organization for Nuclear Research (CERN). (Antiprotons could be trapped only when the large observed shift in energy was compensated.) The uncertainties could be greatly reduced if more antiprotons were allocated for such studies, especially if protons and antiprotons were compared relatively quickly, offering the possibility of more rigorous tests of various theories.

Barkas and co-workers[6] first used emulsion track studies to observe the difference between the energy-loss process for π^+ and π^-, and also for Σ^+ and Σ^-. This effect is now interpreted as being due to polarization of the target material which depends upon the sign of the charge. For a particle of charge Z and velocity v passing through a target of atomic number Z_t, the stopping power S may be written as

$$S=-\frac{dE}{dx}=\frac{4\pi e^4}{mv^2}\frac{N_0}{A}Z^2Z_t(L_0+L_1Z+L_2Z^2)\,. \qquad (1)$$

Here, N_0 is Avogadro's number, m is the electron mass, and A is the atomic number of the target material. The dependence upon the projectile charge Z is characterized by the functions L_0, L_1, and L_2, which depend upon the projectile velocity and the target material. Both the leading term, proportional to L_0 and Z^2, and the next even order term, proportional to L_2 and Z^4, are independent of the sign of Z. A nonzero L_1, however, indicates a Z^3 dependence of the stopping power which is different in sign for projectiles of opposite charge. A positive L_1 indicates more energy loss, and hence a smaller range, for a positive particle than for a negative particle, all other conditions being equal.

The measurements reported here illustrate how studies of the Barkas effect can be carried out when projectiles differing only in sign of charge are sent through the same material. With protons and antiprotons of the same energy, observed differences in the stopping power and range arise only from L_1 (and higher-order terms odd in Z, neglected here) and not from differences in mass or velocity. The effect of the terms of even order in Z cancel. Available experimental data with positive and negative muons[7,8] and with a series of positive ions[9] so far indicate that L_1 is positive. Theoretical investigations[10] agree qualitatively. However, current analytical results differ by approximately a factor of 2, with additional and larger discrepancies arising from numerical calculations.

The apparatus used (Fig. 1) is similar to the apparatus we used with 21-MeV antiprotons several years ago.[11] Antiprotons or protons with a fixed kinetic energy of 5.9 MeV, extracted from LEAR through a thin titanium window, enter this apparatus from below at a rate kept less than 3 kHz. To vary the energy of the projectiles by a small amount, they are sent through two gas cells indicated in Fig. 1. Either SF_6 or N_2 at a pressure of 1 atm was kept flowing slowly through gas cell 1. The energy loss in the N_2 was smaller than the energy loss in the SF_6 by approximately 250 keV, so the energy of the protons and antiprotons leaving gas cell 1 could be changed discontinu-

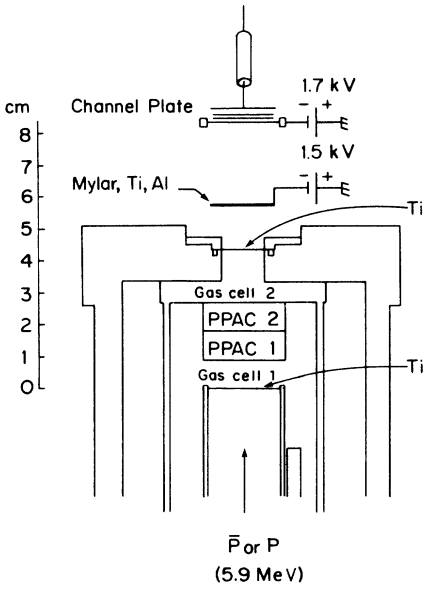

FIG. 1. Time-of-flight apparatus.

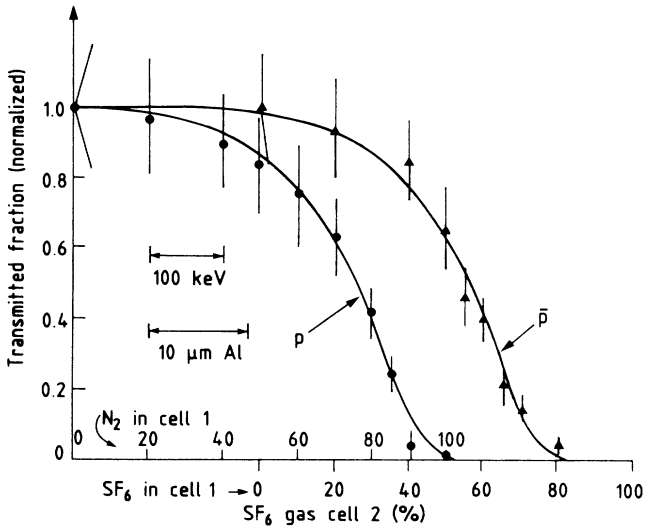

FIG. 2. Normalized fraction of antiprotons detected after the degrader showing the difference in energy loss and range of protons (left) compared to antiprotons (right). The horizontal scale indicates the gas mixture (% by number) used to tune the energy of the proton beam. The size of equivalent changes in the energy of the incident particles and the thickness of the aluminum degrader are indicated by the arrows.

ously by this amount. A mixture of SF_6 and He, also at 1 atm, was sent through gas cell 2. The mix could be adjusted continuously with electronically controlled flow meters, allowing the energy of the antiprotons leaving gas cell 2 to be continuously adjustable over an additional 500 keV when the number of molecules in the mixture was changed from 0% SF_6 (i.e., 100% He) to 100% SF_6 (i.e., 0% He). These energy shifts were calibrated using the variable energy proton beam of a tandem accelerator to produce range curves such as those in Fig. 2. This will be discussed later in the paper. The energy loss was linear in the percentage of SF_6.

Two parallel-plate avalanche counters (PPAC) located between the two gas cells determine when a proton or antiproton enters the apparatus with near unit efficiency and nanosecond resolution. Each detector is composed of five strips oriented in the two transverse directions to provide a position sensitive readout of the beam position with 2.5 mm resolution. Typically, the beam is focused into a spot diameter less than 6 mm (full width half maximum). An active coincidence of the center strips in each PPAC makes is possible to select only protons or antiprotons that pass through a square of side 2.5 mm, centered on the vertical symmetry axis of the apparatus, to avoid counting poorly steered particles. The antiprotons slow in several layers of material needed for the trapping experiments being prepared. (For example, vacuum windows and radiation shields are required to allow cooling of the apparatus to 4.2 K.) Each layer is listed in order in Table I, along with the equivalent thickness of aluminum and the approximate energy loss in each layer.[12] The antiprotons stop and are detected with near unit efficiency in a channel plate detector located several centimeters down beam. The final degrader window and the channel plate are biased as indicated to minimize the probability of detecting a secondary electron liberated from the aluminum. The number of coincidences of the PPAC detectors with the channel plate are divided by the number of PPAC counts to give a measure of the fraction of the incident particles transmitted through the degraders between. Time-of-flight spectra for the transmitted particles are also recorded, making it possible to compare the energy spectra of the transmitted protons and antiprotons. As shown in Table I, most of the slowing, nearly 4 MeV, occurs in the final aluminum layer.

The points in Fig. 2 represent two measurements of the number of transmitted projectiles versus the effective thickness of the degrader. The left curve is for protons, the right curve is for antiprotons. The vertical scale is

TABLE I. Matter traversed by protons and antiprotons.

Material	Equivalent thickness of Al[a] (μm)		Energy loss[a] (MeV)	
10-μm-thick Ti	16		0.21	
Gas cell 1 with N_2	4.4		0.06	
with SF_6		23		0.31
PPAC 1	11		0.16	
PPAC 2	11		0.16	
Gas cell 2 with He	1.4		0.02	
with SF_6		34		0.52
10-μm-thick Ti	16		0.24	
51-μm-thick Mylar	31		0.52	
10-μm-thick Ti	16		0.27	
117-μm-thick Al	117		3.70	
Total	224	275	5.34	6.09

[a]Reference 12.

proportional to the coincidence signal divided by the number of incident projectiles, as described earlier. A small and flat pion background of $\approx 10\%$ (from annihilation pions striking the channel plate) was subtracted off in the case of the antiprotons. The horizontal scale indicates the fraction of SF_6 in gas cell 2 with either N_2 in the first gas cell (tick marks above the axis) or with SF_6 in the first gas cell (tick marks below the axis). The horizontal scale thus essentially represents the "thickness" of the degrader. Increasing the aluminum thickness by 51 μm would cover the same range covered by this scale. Alternatively, the horizontal scale represents the relative energy of the particles incident on the degraders. The entire horizontal scale corresponds to a shift of approximately 750 keV in the incident energy. The shift of the proton range curve as a function of incident proton energy was used to calibrate the gas cells.

The error bars on the measured points in Fig. 2 represent the largest variations observed in the measured points over several hours. These variations were observed to be correlated with beam intensity, beam steering, etc., and could certainly be reduced with beam time devoted to this purpose. The size of the points themselves represent the short-term repeatability over several minutes. The proton and antiproton curves have a similar shape, as illustrated by the identical smooth curves sketched through the measured points, but the antiproton curve is shifted by 150 ± 20 keV. Several corrections and additional uncertainties must be included. The LEAR staff measured the difference in beam energy between protons and antiprotons extracted from LEAR to be 13 ± 12 keV. Temperature differences in the degraders between the proton and antiproton measurements contribute 31 ± 12 keV. Uncertainties in the calibrations of the first and second gas cell contribute ± 30 and ± 20 keV, respectively.[13] The net result is that the energy lost by 5.9 MeV protons is greater by

$$\Delta E = 194 \pm 45 \text{ keV} \tag{2}$$

than the energy lost by 5.9 MeV antiprotons. The aluminum equivalent for this energy difference is $\Delta R = 14$ μm and

$$\frac{\Delta R}{R} = 5.6 \pm 1.4\% \tag{3}$$

is the equivalent fractional range difference in aluminum, the range being larger for antiprotons.

To quote the above range difference for aluminum and to compare with theoretical values, we initially model our degrader as a piece of aluminum approximately 250-μm thick. This is the sum of the equivalent Al thicknesses from Table I. The formula given by the theory of Ashley, Ritchie, and Brandt[14] (ARB) gives a fractional range difference of 3.2%, which is somewhat lower than our measured value. However, Lindhard included the contributions from close collisions which are absent in ARB theory and estimated that the Barkas effect was approximately twice that of ARB theory.[15] To accommodate this effect, Ritchie and Brandt[16] adjusted their original choice of cutoff at small impact parameters to make the L_1 larger. Both the Lindhard theory and the adjusted ARB theory seem to agree with our measurement, though more precise theoretical predictions are clearly needed. To check the simplifying model above, we use the Lindhard theory to estimate that modeling the matter traversed by the beam as a single piece of aluminum could cause an error as large as ± 20 keV, somewhat smaller than the uncertainty from other sources. Thus we can consider Eq. (2) to be the measured energy loss in Al, provided the quoted uncertainty is increased to ± 50 keV. The reason that the Barkas effect occurs primarily in the aluminum is that until they enter the final aluminum degrader at approximately 4 MeV (Table I), both the antiprotons and protons travel rapidly enough so that contributions to the Barkas effect are small.

In summary, the Barkas effect is detected when 5.9-MeV protons and antiprotons are sent through the same aluminum degrader. Because the proton and antiproton differ only in charge, not in either mass or velocity, the Barkas effect is directly measured. Because of the limited beam time for this measurement, the uncertainties are entirely systematic and could be reduced substantially.

We are grateful to CERN and the excellent LEAR staff for providing the protons and antiprotons for this measurement. Calibration of the gas cell and other tests with protons were performed at the tandem accelerator of the University of Washington. This work was supported by the National Science Foundation, the National Bureau of Standards, the U.S. Air Force Office of Scientific Research, the U.S. Department of Energy, and the Bundesministerium für Forschung und Technologie.

*Present address: National Institute of Standards and Technology, Gaithersburg, MD 20899.

†Present address: Institute for Boson Studies, Pasadena, CA 91107.

[1] W. Brandt and G. Basbas, Phys. Rev. A **27**, 578 (1983).

[2] L. H. Andersen, P. Hvelplund, K. Knudsen, S. P. Møller, K. Elsener, K.-G. Rensfelt, and E. Uggerhøj, Phys. Rev. Lett. **57**, 2147 (1986); Phys. Rev. A **36**, 3612 (1987).

[3] R. E. Olsen and T. J. Gay, Phys. Rev. Lett. **61**, 302 (1988).

[4] M. Kimura and M. Inokuti, Phys. Rev. A **38**, 3801 (1988).

[5] G. Gabrielse, X. Fei, K. Helmerson, S. L. Rolston, R. Tjoelker, T. A. Trainor, H. Kalinowsky, J. Haas, and W. Kells, Phys. Rev. Lett. **57**, 2504 (1986).

[6] W. H. Barkas, W. Birnbaum, and F. M. Smith, Phys. Rev. **101**, 778 (1956); W. H. Barkas, J. N. Dyer, H. H. Heckman, Phys. Rev. Lett. **11**, 26 (1963).

[7] W. Wilhelm, H. Daniel, and F. J. Hartmann, Phys. Lett. **98B**, 33 (1981).

[8] A. R. Clark, R. C. Field, H. J. Frisch, W. R. Holley, R. P. Johnson, L. T. Kerth, R. C. Sah, and W. A. Wenzel, Phys. Lett. **41B**, 229 (1972).

[9] H. H. Andersen, H. Simonsen, and H. Sørensen, Nucl. Phys. **A125**, 171 (1969); H. H. Andersen, J. F. Bak, H. Knudsen, and B. R. Nielsen, Phys. Rev. A **16**, 1929 (1977).

[10]Reviewed by G. Basbas, Nucl. Instrum. Methods **B4**, 227 (1984).

[11]The Barkas effect is relatively smaller and more difficult to observe at this higher incident energy. A brief account is in G. Gabrielse, X. Fei, L. Haarsma, S. L. Rolston, R. Tjoelker, T. A. Trainor, H. Kalinowsky, J. Haas, and W. Kells, Phys. Scr. **T22**, 36 (1988).

[12]From L. C. Northcliffe and R. F. Schilling, Nucl. Data Tables A **7**, 233 (1970).

[13]The calibration was actually somewhat better, except initial trouble with a constriction in the gas lines increased the pressure in a gas cell, shifting the range curve. We have increased the uncertainty to include the largest shift we observed.

[14]J. C. Ashley, R. H. Ritchie, and W. Brandt, Phys. Rev. B **5**, 2393 (1972); Phys. Rev. A **8**, 2402 (1973).

[15]J. Lindhard, Nucl. Instrum. Methods **132**, 1 (1976).

[16]R. H. Ritchie and W. Brandt, Phys. Rev. A **17**, 2102 (1978).